

Fig. 3 Stresses at the midsurface of the adhesive layer.

meaningful results. The numerical solutions also reveal the fact that the improperly designed multilayered construction will not produce stress wave attenuation.

#### References

- <sup>1</sup> Postma, G. W., "Wave Propagation in a Stratified Medium," *Geophysics*, Vol. 20, Oct. 1955, pp. 780-806.
- <sup>2</sup> Achenbach, J. D. and Zerbe, T. R., "Flexural Vibrations of Laminated Plate," *Journal of the Engineering Mechanics Division, ASCE*, Vol. 97, June 1971, pp. 619-628.
- <sup>3</sup> Lai, Y. S. and Achenbach, J. D., "Optimal Design of Layered Structures under Dynamic Loading," *Computers and Structures*, Vol. 3, May 1973, pp. 559-572.

## Sweep Effects on Supersonic Separated Flows—A Numerical Study

M. J. WERLE,\* V. N. VATSA,† AND S. D. BERTKE†  
University of Cincinnati, Cincinnati, Ohio

#### Introduction

IN the past several years, considerable success has been achieved in numerically solving the two-dimensional laminar boundary-layer equations when separation occurs in supersonic

flow.<sup>1-5</sup> To date, only a relatively few papers have appeared which address the three-dimensional separation problem due to the highly complex nature of the flowfield. Contained herein is a brief report on recent successes achieved in the numerical solution of the laminar boundary-layer equations for flow past a swept compression ramp in a Mach 3 freestream. The purposes of this study were to assess the influence of boundary-layer cross flow on the numerical algorithm used for two-dimensional separated flows,<sup>4</sup> to take a first step at extending the two-dimensional separated boundary-layer/inviscid flow interaction model to three dimensions, and to inspect the influence of cross flow on heat-transfer levels in the separation and reattachment regions. The approach taken here is wholly numerical, with finite-difference solutions to the boundary-layer equations (modified to account for interaction with inviscid stream) presented for angles of sweep of 0°, 20°, and 45°.

#### Governing Equations

The governing equations employed are the classical three-dimensional equations here simplified for constant cross flow and written in terms of the nondimensional Levy-Lees type variables (see Ref. 6 for the nondimensionalization scheme)

$$\xi = \int_0^s \rho_e \mu_e U_e ds \quad \eta = \frac{U_e}{(2\xi)^{1/2}} \int_0^N \rho dN \quad (1)$$

and the dependent variables

$$F = u/U_e, \quad G = w/W_e, \quad (2a)$$

$$\theta = T/T_e, \quad l = \rho\mu/\rho_e\mu_e \quad (2b)$$

The governing equations become<sup>6</sup>

Longitudinal momentum:

$$(lF_\eta)_\eta - VF_\eta + \beta(\theta - F^2) - 2\xi FF_\xi = 0 \quad (3a)$$

Cross Flow momentum:

$$(lG_\eta)_\eta - VG_\eta - 2\xi FG_\xi = 0 \quad (3b)$$

Energy:

$$(l\theta_\eta)_\eta / Pr - V\theta_\eta + \alpha_1 F_\eta^2 + \alpha_2 G_\eta^2 - 2\xi F\theta_\xi = 0 \quad (3c)$$

Continuity:

$$V_\eta + F + 2\xi F_\xi = 0 \quad (3d)$$

The viscosity function  $l$  is given by Sutherland's law and the inviscid parameters,  $\beta$ ,  $\alpha_1$ , and  $\alpha_2$  are defined as

$$\beta = (2\xi/U_e) dU_e/d\xi \quad (4a)$$

$$\alpha_1 = (1 - 1/\gamma) U_e^2/T_e, \quad \alpha_2 = (1 - 1/\gamma) W_e^2/T_e \quad (4b)$$

These latter quantities depend on the boundary-layer solution through the interaction of the viscous layer growth with the inviscid streamlines. In essence, the boundary layer displays an "effective body" shape—the displacement surface—to the inviscid mainstream over which the inviscid properties must be computed. For present purposes, linearized supersonic flow with constant cross flow is used to relate the local pressure to the slope of the displacement surface  $\phi$  through the relation

$$p_e = p_\infty + \frac{\cos^2 \Lambda}{(M_\infty^2 \cos^2 \Lambda - 1)^{1/2}} \phi \quad (5)$$

where  $\tan \Lambda = W_e/U_e$  is the sweep angle. The isentropic relations provide the remaining inviscid edge quantities and it remains only to relate  $\phi$  to the boundary-layer growth. The total surface inclination includes that induced by the boundary layer as added to the local surface value. In this study, an analytical compression ramp (as shown in Fig. 1) was employed as a "smoothed" version of the typical wedge type configuration employed in experimental separation studies. The ramp angle of approximately 11° was used here since the zero sweep solutions were already available for comparison in Ref. 4. To formally determine the contribution of the boundary-layer growth to the displacement surface angle  $\phi$ , arguments originating in higher order boundary-layer theory are invoked. For regions of nonseparated flows, extension of higher order boundary-layer theory to three dimensions can be shown to locate the inviscid stream surface at a small distance from the surface which exactly corresponds

Received April 12, 1973; revision received July 9, 1973. This research was supported by the Aerospace Research Laboratories under Contract F33615-73-C-4014 and the Naval Air Systems Command under Contract N00019-72-C-0136.

Index categories: Boundary Layers and Convective Heat Transfer—Laminar; Jets, Wakes, and Viscid-Inviscid Flow Interactions.

\* Associate Professor, Department of Aerospace Engineering, Associate Member AIAA.

† Research Assistant, Department of Aerospace Engineering.

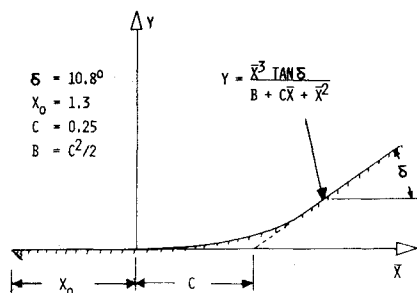


Fig. 1 Ramp geometry.

to the usual displacement thickness definitions (see Moore, Ref. 7 for a physical definition of the displacement body and Werle and Davis, Ref. 8 for an approach based on the method of inner and outer expansions that can be generalized to three dimensions and exactly reproduces Moore's results).

For present purposes the surface angle  $\phi = \theta_s + \epsilon \delta^*/ds$  where  $\theta_s$  is the surface inclination,  $\epsilon = (Re_s)^{-1/2} = (\mu(T_r)/\rho_\infty U_\infty L)^{1/2}$  where  $T_r = U_\infty^2 R$ , and  $\delta^*$  is given by

$$\delta^* = \int_0^\infty \left(1 - \frac{\rho u}{\rho_e U_e}\right) dN = \frac{(2\xi)^{1/2}}{\rho_e U_e} \int_0^\infty (\theta - F) d\eta \quad (6)$$

The above boundary-layer equations were solved using an implicit finite-difference scheme (see Ref. 4 for details) in an iterative manner such that the local inviscid stream, as represented by Eqs. (4-6), was completely compatible with the local displacement body growth. The numerical procedure followed is quite similar to that initiated by Blottner and Flügge-Lotz<sup>9</sup> and as extended by Reyhner and Flügge-Lotz,<sup>3</sup> and Werle and Bertke<sup>10</sup> for separated flows. One new element added here is the cross flow momentum equation, which couples to the usual equation set only through the dissipation term in the energy equation. The numerical solution process is an iterative one with two main iteration processes involved. The first process considers the simultaneous solution of the inviscid and viscous models at a given station along the surface. This is performed here by guessing the inviscid edge quantities ( $p_e$ ,  $\rho_e$ ,  $U_e$ , etc.) at a given station, which allows solution of the boundary-layer equations thus computation of a displacement thickness  $\delta^*$ . This displacement thickness is used to recompute the inviscid edge quantities for comparison with the initial guessed values. This iterative process continued at each station until the guessed and calculated values of all inviscid quantities ceased to change with further iteration.

The second iteration process involves the choice of initial conditions for the boundary-layer equation. With the admitted presence of separated flow regions, account must be made of upstream propagation of downstream effects. In essence, the problem is ill-posed as an initial value problem (see Garvine<sup>11</sup>) and must be solved using a "shooting" technique. Following the usual scheme, the pressure at the initial station is iterated on until

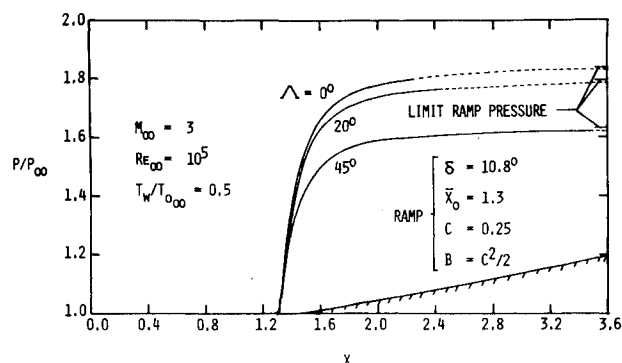


Fig. 2 Influence of sweep on inviscid pressure distributions.

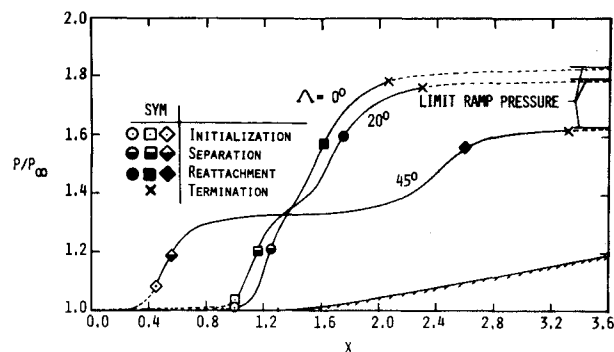


Fig. 3 Influence of sweep on surface pressure distributions.

a downstream compatibility condition is met, here taken to be the return of the surface pressure level to its inviscid value.

### Results and Discussion

Solutions were obtained for the case of a freestream Mach number of 3, Reynolds number of  $10^5$ , and static temperature of  $100^\circ\text{F}$  over the compression ramp of Fig. 1 held at a constant wall temperature ratio  $T_w/T_{0_\infty} = 0.5$ . Results for sweep angles of  $0^\circ$ ,  $20^\circ$ , and  $45^\circ$  corresponding to the inviscid pressure distribution of Fig. 2 are presented here. Note that the pressure distributions for this geometry reasonably well approximate those usually encountered using wedge type compression surfaces. The surface pressure levels produced when the boundary layers separated ahead of these ramps are shown in Fig. 3 where a steady progression of the separation point forward of the ramp point is observed as cross flow increases. In these figures, the point where the calculations are initiated is marked by open symbols, the separation point by a half-filled symbol, the reattachment point by the fully filled symbol and the terminal point in the calculations by a cross. It is only necessary to carry these solutions far enough downstream to assure the position of reattachment to some acceptable degree (say to plotting accuracy) but here the criterion used was that the level of peak reattachment heat transfer be determined within plotting accuracy. The dashed portions of the curves represent speculation as to how the parameters vary outside the range of computation and are only shown for comparison purposes. The skin-friction distributions (note here  $C_f = \tau_w/\rho_\infty U_\infty^2$ ) accompanying these pressure distributions are given in Fig. 4 and are seen to show dramatic excursions from the usual square root decay (dashed lines) of skin friction expected far upstream and downstream of the corner. For all angles of sweep boundary-layer solutions without interaction effects would have incorrectly followed the square root decay up to the corner ( $x = 1.3$ ) followed by a rapid drop in skin friction on the ramp face to a singularity ridden approach to the zero shear point<sup>12-14</sup> and could not be continued aft of separation. Accounting for interaction effects allows the correct upstream propagation of disturbances and a nonsingular pass through the separation and reattachment point back to the square root decay of skin friction along the constant

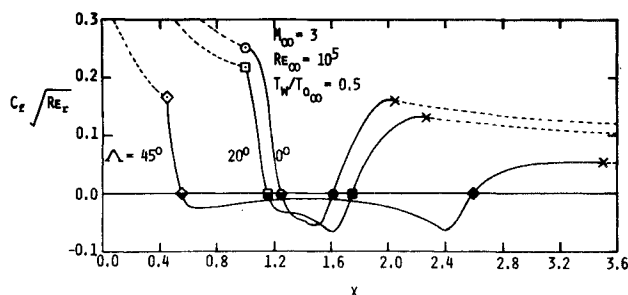


Fig. 4 Influence of sweep on skin-friction distributions.

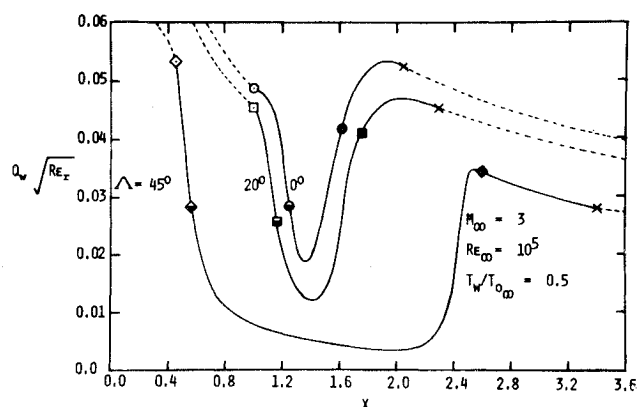


Fig. 5 Influence of sweep on heat-transfer distributions.

pressure region of the ramp. The surface heat-transfer distributions (note here  $Q_w = q_w / \rho_\infty U_\infty^3$ ) accompanying these cases are shown in Fig. 5 to undergo excursions qualitatively similar to those of Fig. 4.

The over-all influence of sweep was quite surprising, it being expected that as the ramp was swept away from the mainstream direction (cross flow increased), the separation bubble would collapse to its ultimate configuration of zero pressure rise with zero separation bubble length. Contrary to this it seems that the flow appears to be approaching a state in which the separation bubble steadily increases in extent as the sweep increases, at least up to  $45^\circ$  of sweep. This is apparently directly connected with the decrease in the normal flow Mach number from 3 at zero sweep to approximately 2 at  $45^\circ$  of sweep. Free interaction studies (see Lewis et al.,<sup>15</sup> Stewartson and Williams,<sup>16</sup> and Werle, Polak and Bertke<sup>4</sup>) for the two-dimensional problem, indicate that lowering  $M_\infty$  should cause an increase in the interaction scale of a separated region for a fixed pressure rise. Here, this scale effect apparently is strong enough to counter the effect of decreasing pressure rise with increased sweep. One would expect that eventually this latter effect would dominate, possibly once the normal Mach number goes subsonic, but the present linearized supersonic flow model cannot be employed to investigate such a limit condition.

One final point of interest is the influence of cross flow on the reattachment heating levels. Of immediate interest is that the peak heating point is generally aft of the reattachment point and that the levels achieved do not seem to show much "overheating." This latter point though really depends strongly on the basis of comparison being used. Consider the peak heat-transfer level observed for  $\Lambda = 0$ , given by  $Q_w = 0.054$  at  $x = 1.95$ . At the same point without the ramp present the heating level would have been 0.036 based on a square root decay from the value of 0.049 shown for  $x = 1.0$ . Thus, the ramp might be said to cause a local heating level 50% higher than its flat plate value. For sweep angle of  $20^\circ$  the overheating remains near 50% and this increases to 55% for  $45^\circ$  of sweep.

#### References

- 1 Lees, L. and Reeves, B. L., "Supersonic Separated and Reattaching Laminar Flows: I—General Theory and Application to Adiabatic Boundary-Layer/Shock-Wave Interaction," *AIAA Journal*, Vol. 2, No. 11, Nov. 1964, pp. 1907–1920.
- 2 Nielsen, J. N., Lynes, L. L., and Godwin, F. K., "Theory of Laminar Separated Flows on Flared Surfaces Including Supersonic Flow with Heating and Cooling," *AGARD Conference Proceedings No. 4: Separated Flows*, 1966.
- 3 Reyhner, T. A. and Flügge-Lotz, I., "The Interaction of a Shock Wave with a Laminar Boundary Layer," Rept. 163, Nov. 1966, Div. of Engineering Mechanics, Stanford Univ., Stanford, Calif.
- 4 Werle, M. J., Polak, A., and Bertke, S. D., "Supersonic Boundary-Layer Separation and Reattachment—Finite Difference Solutions," Rept. AFL 72-12-1, Jan. 1973, Univ. of Cincinnati, Aerospace Engineering Dept., Cincinnati, Ohio.

5 Dwyer, D. L., "Supersonic and Hypersonic Two-Dimensional Laminar Flows Over a Compression Corner," paper presented at AIAA Computational Fluid Dynamics Conference, Palm Springs, Calif., July 16–18, 1973.

6 Vatsa, V. N. and Davis, R. T., "The Use of Levy-Lees Variables in Three-Dimensional Boundary-Layer Flows," CR 112315, 1973, NASA.

7 Moore, F. K., "Displacement Effect of a Three-Dimensional Boundary Layer," TN-2722, 1952, NACA.

8 Werle, M. J. and Davis, R. T., "Integral Equations for Incompressible Second-Order Boundary Layers," *International Journal of Engineering Sciences*, Vol. 4, 1966, pp. 423–431.

9 Flügge-Lotz, I. and Blottner, F. G., "Computation of the Compressible Laminar Boundary Layer Flow Including Displacement Thickness Interaction Using Finite Differences Methods," TR 131, 1962, Div. of Engineering Mechanics, Stanford Univ., Stanford, Calif.

10 Werle, M. J. and Bertke, S. D., "A Finite-Difference Method for Boundary Layers with Reverse Flow," *AIAA Journal*, Vol. 10, No. 9, Sept. 1972, pp. 1250–1252.

11 Garvine, R. W., "Upstream Influence in Viscous Interaction Problems," *The Physics of Fluids*, Vol. 11, No. 7, July 1968, pp. 1413–1423.

12 Brown, S. N. and Stewartson, K., "Laminar Separation," *Annual Review of Fluid Mechanics*, Vol. 1, 1969, pp. 45–72.

13 Buckmaster, J., "Separation and the Compressible Boundary Layer," *Journal of Engineering Mathematics*, Vol. 5, No. 1, 1971, pp. 71–77.

14 Werle, M. J. and Senehal, G. D., "A Numerical Study of Separating Supersonic Laminar Boundary Layers," American Society of Mechanical Engineers, Paper 73-APM-H, *Journal of Applied Mechanics*, 1973.

15 Lewis, J. E., Kubota, T., and Lees, L., "Experimental Investigation of Supersonic Laminar, Two-Dimensional Boundary-layer Separation in a Compression Corner With and Without Cooling," *AIAA Journal*, Vol. 6, No. 1, Jan. 1968, pp. 7–14.

16 Stewartson, K. and Williams, P. G., "Self-Induced Separation," *Proceedings of the Royal Society of London, Ser. A*, Vol. 312, Sept. 1969, pp. 181–206.

## Probe Interference in High-Speed Rarefied Flows

D. M. COGAN\* AND J. K. HARVEY†  
Imperial College, London, England

#### Introduction

HIGH-SPEED flows which lie between the continuum and free molecular regimes have been extensively investigated with pitot probes and heat-transfer probes. It was assumed that as the flowfield is supersonic, probe disturbances are confined to a region downstream of the probe. The present investigation was prompted by anomalous results obtained when momentum flux ( $\rho u^2$ ) and mass flux ( $\rho u$ ) measurements were combined to give density and velocity profiles. These anomalies could only be explained by probe interference, which was confirmed by the independent density measurements described below. The purpose of this Note is to demonstrate that high-speed rarefied flows are disturbed by probes of the size normally used. This disturbance may only become apparent when an independent measurement of flow properties is performed.

#### Experimental Investigation

Measurements were conducted in a continuous running arc heated wind tunnel, using argon gas. The flow in the working

Received April 26, 1973; revision received July 24, 1973.

Index category: Rarefied Flows.

\* Department of Aeronautics; presently Lecturer, King Faisal Air Academy, Riyadh, Saudi Arabia.

† Senior Lecturer, Department of Aeronautics. Member AIAA.